

A Noncanonical Hippo Pathway Regulates Spindle Disassembly and Cytokinesis During Meiosis in *Saccharomyces cerevisiae*

Scott M. Paulissen,^{*1} Cindy A. Hunt,^{*} Brian C. Seitz,^{*} Christian J. Slubowski,^{*2} Yao Yu,^{†,3} Xheni Mucelli,^{*} Dang Truong,^{*4} Zoey Wallis,^{*} Hung T. Nguyen,^{*5} Shayla Newman-Toledo,^{*} Aaron M. Neiman,[†] and Linda S. Huang^{*6}

^{*}Department of Biology, University of Massachusetts Boston, Massachusetts 02125 and [†]Department of Biochemistry and Cell Biology, Stony Brook University, New York 11794

ORCID IDs: 0000-0002-9258-2380 (S.M.P.); 0000-0003-1901-1052 (B.C.S.); 0000-0002-6600-6996 (A.M.N.); 0000-0002-9033-4391 (L.S.H.)

ABSTRACT Meiosis in the budding yeast *Saccharomyces cerevisiae* is used to create haploid yeast spores from a diploid mother cell. During meiosis II, cytokinesis occurs by closure of the prospore membrane, a membrane that initiates at the spindle pole body and grows to surround each of the haploid meiotic products. Timely prospore membrane closure requires *SPS1*, which encodes an STE20 family GCKIII kinase. To identify genes that may activate *SPS1*, we utilized a histone phosphorylation defect of *sps1* mutants to screen for genes with a similar phenotype and found that *cdc15* shared this phenotype. *CDC15* encodes a Hippo-like kinase that is part of the mitotic exit network. We find that *Sps1* complexes with *Cdc15*, that *Sps1* phosphorylation requires *Cdc15*, and that *CDC15* is also required for timely prospore membrane closure. We also find that *SPS1*, like *CDC15*, is required for meiosis II spindle disassembly and sustained anaphase II release of *Cdc14* in meiosis. However, the NDR-kinase complex encoded by *DBF2/DBF20 MOB1* which functions downstream of *CDC15* in mitotic cells, does not appear to play a role in spindle disassembly, timely prospore membrane closure, or sustained anaphase II *Cdc14* release. Taken together, our results suggest that the mitotic exit network is rewired for exit from meiosis II, such that *SPS1* replaces the NDR-kinase complex downstream of *CDC15*.

KEYWORDS sporulation; gametogenesis; STE20 family-GCKIII kinase; meiosis; cell cycle control

SEXUAL reproduction requires meiosis for the production of haploid gametes from a diploid precursor cell. The events of meiosis, such as spindle disassembly and cytokinesis, must be properly coordinated along with the developmental events that occur during gametogenesis. A better understanding of

how these events are coordinated is important for understanding gamete formation.

In the budding yeast *Saccharomyces cerevisiae*, the haploid gametes are spores, which form when diploid cells encounter starvation conditions where nitrogen and carbon are limiting [reviewed in Neiman 2011]. During sporulation, the diploid mother cell remodels its interior to form four haploid spores. Spore morphogenesis begins with the formation of a prospore membrane that grows from the spindle pole body. The prospore membranes grow around the haploid nuclei and fuse to close at the side of the nucleus away from the spindle pole body, resulting in the capture of each nucleus within its own membrane (Diamond *et al.* 2009). A protein complex known as the Leading Edge Protein complex is at the growing edge of the prospore membrane and includes *Ssp1*, *Ady3*, *Irc10*, and *Don1* (Knop and Strasser 2000; Moreno-Borchart *et al.* 2001; Nickas and Neiman 2002; Maier *et al.* 2007; Lam *et al.* 2014).

Prospore membrane closure is the cytokinetic event in meiosis and involves the removal of the Leading Edge Protein complex (Maier *et al.* 2007). Proper timing of prospore membrane

Copyright © 2020 by the Genetics Society of America
doi: <https://doi.org/10.1534/genetics.120.303584>

Manuscript received December 19, 2019; accepted for publication August 9, 2020; published Early Online August 11, 2020.

Supplemental material available at figshare: <https://doi.org/10.25386/genetics.12774536>.

¹Present address: National Institute of Child Health and Human Development, National Institutes of Health, 9000 Rockville Pike, Bethesda, MD 20892.

²Present address: LakePharma, Inc., 35 South Street, Hopkinton, MA 01748.

³Present address: State Key Laboratory of Genetic Engineering, School of Life Science, Fudan University, 220 Handan Rd, Wu Jiao Chang, Yangpu District, Shanghai 200438, China.

⁴Present address: Department of Chemistry, University of Massachusetts Lowell, 220 Pawtucket St, Lowell, MA 01854.

⁵Present address: Henry M. Goldman School of Dental Medicine, Boston University, 635 Albany St., Boston, MA 02215.

⁶Corresponding author: Linda S. Huang, Department of Biology, University of Massachusetts Boston, 100 Morrissey Blvd., Boston, MA 02125. E-mail: linda.huang@umb.edu

closure requires *SPS1*, which encodes an STE20 family GCKIII kinase; cells lacking *SPS1* produce hyperelongated prospore membranes that close later than those in wild-type cells (Slubowski *et al.* 2014; Paulissen *et al.* 2016). Prospore membrane closure must be properly coordinated with other meiosis II events, such as spindle disassembly.

Compared to meiosis, exit from mitosis, which involves the downregulation of CDK activity and the coordination of spindle disassembly and cytokinesis, has been more extensively studied. Mitotic exit involves the activation of the *Tem1*-GTPase at the spindle pole body as it moves into the newly formed bud, leading to the activation of the *Cdc15* Hippo-like kinase (Mah *et al.* 2001; Visintin and Amon 2001; D'Aquino *et al.* 2005; Pereira and Schiebel 2005; Maekawa *et al.* 2007; Chan and Amon 2010; Bertazzi *et al.* 2011; Rock and Amon 2011; Falk *et al.* 2016). *Cdc15* phosphorylates the spindle pole body localized *Nud1* scaffold, which leads to the recruitment and activation of the NDR kinase complex, *Dbf2-Mob1* (Gruneberg *et al.* 2000; Luca *et al.* 2001; Rock *et al.* 2013). A decrease in mitotic cyclin-dependent kinase (CDK) activity is also required for *Cdc15* and *Mob1* activation (Campbell *et al.* 2019). Activation of the NDR kinase complex promotes the sustained release of the *Cdc14* serine-threonine phosphatase from the nucleolus, to inactivate mitotic CDK activity and promote exit from mitosis (Visintin *et al.* 1998; Shou *et al.* 1999; Mohl *et al.* 2009; Manzoni *et al.* 2010). These components are part of the mitotic exit network (MEN) [reviewed in Bardin and Amon 2001; Stegmeier and Amon 2004; Hergovich and Hemmings 2012; Weiss 2012; Juanes and Piatti 2016; see Figure 1A].

Meiotic exit uses some, but not all of the MEN components. Exit from meiosis I does not require the MEN (Kamieniecki *et al.* 2005; Pablo-Hernando *et al.* 2007; Attner and Amon 2012), which instead acts to coordinate exit from meiosis II. *CDC15* plays a role in meiosis II spindle disassembly (Pablo-Hernando *et al.* 2007; Attner and Amon 2012) and is also required to maintain nuclear and nucleolar release of *Cdc14* in meiosis II (Pablo-Hernando *et al.* 2007). Furthermore, a prospore membrane closure (Diamond *et al.* 2009) and morphology (Pablo-Hernando *et al.* 2007) defect have been described for *cdc15*. However, the upstream MEN component *TEM1* does not appear to play a role in *Cdc15* activation, as the *Tem1*-GTPase is not seen at the spindle pole body in meiosis (Attner and Amon 2012) and *Tem1*-depleted cells complete meiosis with similar efficiencies to wild-type cells (Kamieniecki *et al.* 2005). The spindle pole body located scaffold encoded by *NUD1* is also likely not involved in exit from meiosis, as *nud1* temperature-sensitive alleles do not disrupt meiosis (Gordon *et al.* 2006) and *NUD1* is not required for *Dbf20* kinase activity in meiosis (Attner and Amon 2012).

In meiosis, the NDR-kinase complex utilizes the *Mob1* regulatory subunit along with either of the paralogous *Dbf20* and *Dbf2* NDR kinases (Attner and Amon 2012; Renicke *et al.* 2017). *MOB1* plays a role in meiosis II, as *mob1* cells progress through meiosis I with wild-type kinetics, but show a delay in exit from meiosis II (Attner and Amon 2012). *Dbf20* kinase is active in meiosis II, and its kinase

activity, as well as its interaction with the *Mob1* regulatory subunit, is dependent on *CDC15* in meiosis II, although deletion of *DBF20* did not show a delay in meiosis II exit (Attner and Amon 2012). The major phenotype seen for cells lacking the NDR kinases complex in meiosis is a defect in spore number control (Renicke *et al.* 2017); spore number control involves the selection of nuclei associated with younger spindle pole bodies over older spindle pole bodies for spore packaging when available energy resources are low (Davidow *et al.* 1980; Nickas *et al.* 2004; Taxis *et al.* 2005). *Nud1* is also involved in spore number control (Gordon *et al.* 2006; Renicke *et al.* 2017). Thus, although the MEN member *CDC15* seems to play a role in exit from meiosis II, it is unclear what other components *CDC15* acts with during meiosis II. *TEM1* and *NUD1* do not appear to play a role in meiosis II and the NDR kinase complex has not been examined for spindle disassembly, prospore membrane closure, and *Cdc14* release (diagrammed in Figure 1A).

Here, we examine timely prospore membrane closure, meiosis II spindle disassembly, and *Cdc14* sustained release in anaphase II, and find that *CDC15* and *SPS1* act together to regulate exit from meiosis II. However, the NDR kinase complex encoded by *DBF2 DBF20 MOB1* does not seem to be involved in these events. Instead, *DBF2 DBF20 MOB1* is important for spore number control, as previously demonstrated (Renicke *et al.* 2017). Likewise, we find that *CDC15* and *SPS1* are not involved in controlling spore number and appear to act separately from the NDR kinase complex in meiosis II.

Materials and Methods

Yeast strains, growth, and sporulation

All strains used in this study are in the SK1 background (Kane and Roth 1974) and are described in Supplemental Material, Tables S1 and S2. All strains are derived from LH177 (Huang *et al.* 2005), except for YS429 (see below), the previously published strains (AN117-4B, A20239, A22416, and HI50), and the published strains used for screening (see below and Table S1 and S3); alleles from these strains were crossed into the LH177-derived SK1 strain background. Standard genetic methods were used to create and propagate strains unless otherwise noted (Rose and Fink 1990). Epitope-tagged strains and knockout alleles were created using PCR-mediated recombination methods, as previously described (Longtine *et al.* 1998; Lee *et al.* 2013; Slubowski *et al.* 2015).

The *SPS1^{K47R-zz}* allele was created by first creating an intermediate strain where the *URA3^{K1}* gene replaced the kinase domain of *SPS1-zz* (LH960; Slubowski *et al.* 2014), using OLH712 (GCAAACCAGCATTTGCTTTAAATTAGTTTTT TACTAGCTAACacaggaaacagctatgc) and OLH775 (GCAAACC AGCATTGCTTTAAATTAGTTTTACTAGCTAACacagg aaacagctatgc) to amplify *URA3^{K1}* (Huang *et al.* 2005). This intermediate strain was then transformed with *SPS1* DNA from a plasmid containing the K47R mutation (Slubowski *et al.* 2014). Transformants were identified through counterselection

on plates containing 5-fluoroorotic acid, as previously described (Huang *et al.* 2005). The genomic DNA from the *sps1*^{K47R}-zz-containing strain was sequenced, to confirm the correct replacement of the catalytic lysine. The *GFP^{ENVY}-TUB1* allele was created using the plasmid *pHIS3p:ENVY-TUB1+3'UTR::LEU2* (described below), which was linearized by BsaBI digest and integrated into the *TUB1* locus [similar to Markus *et al.* (2015)].

The *hho1*::*TRP1*^{C-g} (*hho1Δ*) allele was constructed by amplifying *TRP1*^{C-g} from pCgW using OLH2337 (TTGGCAGC GAGGGAAAGCAATTATAACAACTAAAGCAACcacaggaaacag ctatgacc) and OLH2338 (TTGCTATCACCATTGACATTCTCGTT GGATATTCACTTgttgtaaaacgcacggccagt), which contained homology to the regions flanking the *HHO1* open reading frame, transforming the PCR product into a haploid SK1 strain, and genotyping the transformants by PCR.

YS429 was constructed by replacing the native *DBF2* promoter with the *CLB2* promoter by PCR-mediated integration, using pRK67 (Kamieniecki *et al.* 2005) as a template in strain AN117-4B (Neiman *et al.* 2000). The resulting haploid was crossed to a *dbf20Δ::kanMX6* haploid from the yeast knockout collection (Rabitsch *et al.* 2001), and segregants from this cross were mated to create YS429.

The *CDC15-9MYC* allele in LH1070 and LH1071 is from A22416 (Attner and Amon 2012). The *mob1-mn* (*KanMX6::pCLB2-3HA-MOB1*) allele used in this study is from A20239 (Attner and Amon 2012). The *cdc15-mn* (*mxKAN:prCLB2::HA:CDC15*) allele used in this study is from HI50 (Pablo-Hernando *et al.* 2007).

Unless otherwise noted, cells were grown in standard yeast media and sporulated in a synchronous manner in liquid media, as previously described (Huang *et al.* 2005). In brief, liquid cultures were grown with agitation at 30°. Cells to be sporulated were first grown to saturation in YPD overnight at 30° and then transferred to YPAcetate (yeast extract - peptone - acetate) and grown to ~1.5 OD₆₀₀/ml overnight. These cells were then harvested, washed in double-distilled H₂O, and resuspended in 1% potassium acetate at an OD₆₀₀/ml of 2.0. Sporulation of cells containing plasmids was the same as above, except instead of YPD, cells were grown in synthetic dextrose media, lacking the appropriate nutrient for selection.

Plasmids

The plasmid pRS426-E20 was created by PCR amplification of *GFP^{EnvY}* from pFA6a-link-*GFP^{EnvY}*-SpHIS5 (Slubowski *et al.* 2015) using primers OLH1669 (GTGTggatccATGTCTAAAG GCGAGGAATG) and OLH1679 (GTGTgaattcTTTGTACAA TTCGTCCATTCTCAA), which incorporated the BamHI and EcoRI restriction sites flanking *GFP^{EnvY}*. The amplified fragment was then digested with EcoRI and BamHI. pRS426-G20 (Nakanishi *et al.* 2004) was also digested with EcoRI and BamHI, removing the GFP from in front of the *SPO20* fragment on that plasmid. The resulting linearized backbone was then ligated to the *GFP^{EnvY}* PCR fragment. The resulting plasmid was verified by sequencing.

The plasmid *pHIS3p:ENVY-TUB1+3'UTR::LEU2* was constructed using the backbone from *pHIS3p:yomRUBY2-TUB1+3'UTR::LEU2*

(Markus *et al.* 2015); *yomRUBY2* was replaced by *GFP^{ENVY}* in this plasmid after the addition of the SacI and BamHI restriction sites flanking the fluorescent protein insertion site. *GFP^{ENVY}* was taken from the plasmid pFA6a-link-*GFP^{EnvY}*-SpHIS5 (Slubowski *et al.* 2015). *pHIS3p:ENVY-TUB1+3'UTR::LEU2* was verified by sequencing.

Screening for H4S1p phenotype

To screen for an H4S1p phenotype, mutant strains were inoculated in 20 ml YPD and grown overnight. Cultures were diluted 1:100 into 80 ml YPAcetate, such that the OD₆₀₀ was between 0.1 and 0.2, and grown overnight to reach an OD₆₀₀ between 1.0 and 1.2. Cells were collected, washed in double-distilled H₂O, and resuspended in 50 ml of 2% potassium acetate at an OD₆₀₀ of 1.2 (~2 × 10⁷ cells/ml). Then, 10 ml of cells were collected at 0, 8, 10, and 24 hr after induction of sporulation. Proteins were extracted by resuspending cells in Breaking Buffer (50 mM Tris-HCl, pH 7.5, 10% glycerol, 1 mM EDTA, 10mM MgCl₂, 100mM NaCl, 1 mM DTT) with protease inhibitors (1 mM PMSF, 1 µg/ml leupeptin, 1 µg/ml peptastin A) and phosphatase inhibitors (100 mM NaF, 100 mM Na₄P₂O₇, 10 mM Na₃VO₄). Cells were lysed using glass beads and a bead beater. Protein concentration of extracts was determined using the Bio-Rad Protein Assay, and extracts were adjusted to similar concentrations. Loading buffer was added to extract, which were then boiled and loaded onto an SDS-PAGE gel and immunoblotted. H4S1p was detected using a rabbit anti-phospho-H4/H2A S1p antibody (07-179, Upstate Biotechnology/EMD Millipore) at a dilution of 1:4000, detected using HRP-conjugated secondary antibodies and ECL reagents (Amersham/GE Healthcare), and exposed to X-ray film.

Immunoblotting

For all immunoblotting experiments other than those performed for the H4S1p screening, cells were collected at the indicated times and prepared using the trichloroacetic acid (TCA) precipitation method (Philips and Herskowitz 1998), which involves addition of lysis buffer (1.85 N NaOH and 10% v/v β-mercaptoethanol) followed by precipitation of proteins with 50% (v/v) TCA. Precipitated protein lysates were washed with ice-cold acetone and resuspended in 2× sample buffer neutralized with 5 µl of 1 M Tris base; samples were heated before loading. Protein lysates were separated on standard single percentage SDS-PAGE gels, except for the histone phosphorylation blot in Figure 1A, which was run on a Novex 10–20% Tricine gel (Invitrogen, Carlsbad, CA).

The separated protein extracts were transferred onto an Immobilon low-fluorescence PVDF membrane, blocked with PBS block (LI-COR), and incubated with the appropriate primary antibodies. H4S1 phosphorylation was detected using the anti-phospho-histone H4/H2A S1p antibody at 1:1000 (Upstate Biotechnology/EMD Millipore); sf-GFP-*Sps1* was detected using JL-8 anti-GFP antibodies (Takara/Clontech) at 1:1000; *Sps1-13xmyc* and *Cdc15-9xmyc* were detected using 9E10 anti-myc antibodies (Covance) at 1:1000; *Pgk1* was detected by using 22C5D8 anti-*Pgk1* (Life Technologies) at 1:1000;

fluorescent infrared-dye-conjugated anti-mouse secondary antibodies were used at 1:10,000 (LI-COR). All membranes were imaged using an Odyssey Infrared Imaging System (LI-COR).

Immunoprecipitation

Lysates for immunoprecipitation were prepared from 120 OD₆₀₀ of cells. Cell pellets were lysed in a MiniBeadBeater8 (Biospec) at 4° with glass beads in immunoprecipitation (IP) buffer (300 mM NaCl, 5 mM EGTA, pH 8.0, 50 mM Tris, pH 7.4, and 0.5% Nonidet P-40) with added protease and phosphatase inhibitors, as previously described (Huang *et al.* 2005).

Lysate was clarified with three spins at maximum speed in a tabletop microcentrifuge, and an aliquot was saved for examination by immunoblot; this aliquot was first TCA precipitated before loading onto an SDS-PAGE gel. For immunoprecipitation, clarified lysate was then added to 40 µl of blocked agarose beads (ChromoTek) incubated on a nutator at 4° for 30 min. Lysates incubated on a nutator at 4° for 2 hr with 20 µl of GFP-Trap beads (ChromoTek). GFP-Trap complexes were then washed four times in IP buffer and resuspended in 2× SDS-PAGE sample buffer, boiled for 5 min, clarified through centrifugation, and then separated by SDS-PAGE.

Phos-tag analysis

Phos-tag gels were made using Phos-tag acrylamide (WACO) at a final concentration of 31.4 µM Phos-tag and 50.6 µM MnCl₂ in an otherwise standard 6% SDS-polyacrylamide gel, as described in (Whinston *et al.* 2013). Samples were prepared as above and run at 80 V at 4°, before being transferred and imaged, as above.

Microscopy

Widefield microscopy was performed using a ×100 (NA 1.45) objective on a Zeiss Axioskop Mot2. Images were taken using an Orca-ER cooled CCD camera (Hamamatsu) using Openlab 4.04 (Perkin Elmer, Norwalk, CT) or iVision (BioVision Technologies) for image acquisition. Confocal microscopy was performed using a ×100 (NA 1.49) objective on a Zeiss LSM-880 confocal microscope. Confocal images were acquired using Zeiss Zen-Black software. Images were cropped and merged using ImageJ and FIJI (Schneider *et al.* 2012; Schindelin *et al.* 2012).

Quantitation of prospore membrane morphology

Cells were sporulated and cultures were monitored for prospore membrane development in anaphase II. When cultures were at the stage when prospore membranes should be closing, an experimentalist who did not know the genotype of the culture would score prospore membrane morphology, classifying the prospore membranes into three classes: elongated, closed (by looking for rounded prospore membranes), and hyperelongated.

Assaying prospore membrane closure, formation, and number

Cells were assayed for prospore membrane closure and formation as previously described (Paulissen *et al.* 2016). For prospore

membrane closure and formation, only cells in anaphase II (as determined by *Htb2*-mCherry) were counted. Cells were considered to have initiated prospore membranes if a single prospore membrane could be detected. Cells were considered to have closed their prospore membranes if a single, rounded prospore membrane was detected within the ascus.

To assay the number of prospore membranes that form within the mother cell, cells were sporulated in 1% acetate and fixed using 4.5% methanol-free formaldehyde. Only cells in anaphase II (as determined by *Htb2*-mCherry) were counted. Cells were counted on a Zeiss Axioskop Mot2 using a ×100 (NA 1.45) objective. Strains were sporulated in triplicate; 100 anaphase II cells were counted per culture, for a total of 300 cells per strain. The time at which 50% of cells closed prospore membranes was based on when the average observed time point would have theoretically had 50% closed prospore membranes, and calculated by linear interpolation.

Assaying microtubule morphology

Microtubule morphology was assayed in live sporulating cultures using *GFP^{ENVY}-TUB1*. Images were captured using a Zeiss Axioskop Mot2 with a ×100 (NA 1.45) objective. 3-µm z-stacks with 0.5-µm steps were captured and made into maximal intensity projections for counting spindle fragments. Cells were judged to be in anaphase II by the presence of four distinct nuclei, as visualized using *HTB2*-mCherry.

Statistical analysis

Data were formatted using R version 3.6.3 (February 29, 2020) *Holding the Windsock*, using the Tidyverse packages *tidyverse* and *dplyr*. Graphs were plotted using the package *ggplot2*. For the categorical data in Figure 3, statistical comparison was performed using a chi-square test and pairwise, 2 × 2 Fisher's exact test *post hoc*, Bonferroni-corrected for multiple comparisons. For Figures 4, 5, and 6 and Figures S5 and S6, statistical comparisons were performed by one-way ANOVA followed by Tukey Honest Significant Difference *post hoc* test using JMP11 (SAS).

Data availability

The strains and plasmids created for this study are available upon request. Supplemental material available at figshare: <https://doi.org/10.25386/genetics.12774536>. The data necessary for confirming the conclusions of this article are present.

Results

CDC15 is required for *Sps1* phosphorylation

Phosphorylation of the *Ser1* residue of histone H4 is greatly increased during meiosis, and *Sps1* had previously been demonstrated to be important for this phosphorylation (Krishnamoorthy *et al.* 2006). To identify additional genes that may function with *Sps1*, we used a Western blot assay with a H4/H2A Serine1 phosphorylation (H4/H2A S1p)-specific antibody to initially screen through a few genes involved in sporulation (*ama1*, *cdc15*, *gip1*, *spo71*,

spo73, *spo75*, *spo77*, and *ssp2*) for those that display an H4 phosphorylation defect similar to *sps1Δ* mutants. Because *CDC15* is required in mitotic cells, we used the *cdc15-mn* allele (*cdc15*-meiotic null; *CDC15* under the control of the mitotic *CLB2* promoter) (Lee and Amon 2003; Pablo-Hernando *et al.* 2007) to assay *CDC15* function during sporulation. We then carried out a more unbiased screen, examining H4 phosphorylation in a subset of strains from a collection of mutants in genes that are upregulated in sporulation (Rabitsch *et al.* 2001). The 116 genes that were tested are listed in Table S3. We found that *atg9*, *atg18*, *cdc15*, *mnd2*, *set1*, *spo77*, and *trs85* were among the mutants that decrease histone phosphorylation during sporulation.

SPO77 was isolated as a high-copy suppressor of a hypomorphic allele of *sps1*, and acts with *SPS1* to regulate timely prospore membrane closure in a pathway in parallel to *AMA1* (Paulissen *et al.* 2016); *AMA1* encodes a meiosis-specific activator of the anaphase promoting complex (APC/C) (Cooper *et al.* 2000). We see that *ama1Δ* mutants do not have a histone phosphorylation defect during sporulation (unlike *sps1Δ*, *cdc15-mn*, and *spo77Δ*) consistent with *AMA1* acting separately from the *SPS1* pathway (Figure 1B). Because *CDC15* has been reported to affect prospore membrane closure (Diamond *et al.* 2009) and since a link between *SPS1* and *CDC15* was not previously reported, we focused our studies on better understanding the relationship of *CDC15* and *SPS1*.

Since *Sps1* is a phosphoprotein (Slubowski *et al.* 2014) and because *CDC15* encodes a Hippo-like protein kinase (Schweitzer and Philippse 1991; Rock *et al.* 2013), we asked whether *CDC15* was required for *Sps1* phosphorylation. We examined *Sps1* phosphorylation state in sporulating cells with depleted levels of *Cdc15*. Separation of *Sps1* on an SDS-PAGE gel revealed that the doublet seen in wild-type cells (Slubowski *et al.* 2014) collapses into the faster migrating band in the *cdc15-mn* strain (Figure 1C and Figure S1). This result suggested that much of the post-translational modification of *Sps1* protein was *CDC15* dependent.

To better examine the migration shifts due to post-translational phosphorylation, we used a Phos-tag polyacrylamide gel to resolve the *Sps1* protein. Phos-tag gels specifically retard the migration of phosphorylated protein species through the gel (Kinoshita *et al.* 2006). *Sps1* runs as multiple bands on a Phos-tag gel, consistent with it being a phosphoprotein (Figure 1D). This banding pattern was strikingly reduced in the *cdc15-mn* strain (Figure 1D), which supports the idea that *CDC15* is required for most, if not all, of the phosphorylation of *Sps1*.

To determine whether the phosphorylation of *Sps1* by *Cdc15* may be direct, we examined whether *Cdc15* and *Sps1* physically interact in sporulating cells by co-immunoprecipitation. Using protein lysates from a strain containing both *CDC15-13myc* and *sfGFP-SPS1*, we see *Cdc15* and *Sps1* in a complex (Figure 1E).

Because *Cdc15* is a phosphoprotein (Jaspersen and Morgan 2000; Jones *et al.* 2011), we asked if post-translational modifications of *Cdc15* were altered in *sps1Δ* mutants. SDS-PAGE analysis of *Cdc15* in both wild-type and *sps1Δ* mutant cells both

show a distinct doublet, suggesting that phosphorylation of *Cdc15* is not altered in the *sps1Δ* mutant (Figure S2), consistent with *CDC15* acting upstream of *SPS1*. Taken together, these results show that *CDC15* is required for *Sps1* phosphorylation, and support a model in which *Cdc15* is the upstream activating kinase of *Sps1*.

Like *SPS1*, *CDC15* is required for timely prospore membrane closure

Previous studies have demonstrated a role for *CDC15* in prospore membrane morphogenesis, with *cdc15* mutant cells forming aberrant prospore membrane morphologies (Pablo-Hernando *et al.* 2007) and having a defect in closing prospore membranes (Diamond *et al.* 2009). To visualize prospore membranes, we utilized GFP (either eGFP or GFP^{EnvY}, a bright and photostable GFP variant; Slubowski *et al.* 2015) fused to the 40-amino-acid prospore membrane-targeting region of the *Spo20* protein (Nakanishi *et al.* 2004). We examined prospore membranes in live cells during sporulation in wild-type, *sps1Δ*, and *cdc15-mn* cells. Unlike wild-type cells (Figure 2A), *cdc15-mn* cells show hyperelongated prospore membranes (Figure 2C), similar to those seen in *sps1Δ* cells (Figure 2B), consistent with the previously described *cdc15* prospore membrane morphology (Pablo-Hernando *et al.* 2007) and closure defect (Diamond *et al.* 2009).

We asked whether *SPS1* and *CDC15* acted in the same or in a parallel pathway, to regulate prospore membrane closure. We created the *cdc15-mn* *sps1Δ* strain and saw that the double mutant cells displayed a prospore membrane morphology defect that was no worse than that of either the *sps1Δ* or *cdc15-mn* mutation alone (Figure 2, B–D), consistent with both genes acting in the same pathway.

We quantitated the prospore membrane morphology defect by blind scoring of prospore membranes during late anaphase II, when prospore membranes close in wild-type cells (Figure 3A). We find that *sps1Δ*, *cdc15-mn*, and *cdc15-mn* *sps1Δ* cells all have a significantly greater percentage of cells with hyperelongated prospore membranes compared to wild-type cells ($P < 0.01$), while the percentage cells with hyperelongated prospore membranes in the *cdc15-mn* *sps1Δ* strain did not significantly differ from that seen in *sps1Δ* and *cdc15-mn* single mutants ($P < 0.01$).

Because *SPS1* plays a role in timely prospore membrane closure (Paulissen *et al.* 2016), we asked whether *CDC15* affects the timing of prospore membrane closure. To assay prospore membrane closure, we examined the appearance of rounded prospore membranes, as rounded prospore membranes appear when the membrane closes (Diamond *et al.* 2009; Paulissen *et al.* 2016). Cells with *cdc15-mn* exhibited both a delay in appearance of, as well as a reduction in, the accumulation of closed prospore membranes, forming rounded membranes at $\sim 72\%$ (Figures 2C and 3B), similar to the reduction seen in *sps1Δ* mutants and less than the 95% seen in wild-type cells (Figure 3B). When we calculate when 50% of the prospore membranes close, we see a significant delay of about an hour when comparing *sps1Δ* and *cdc15-mn*

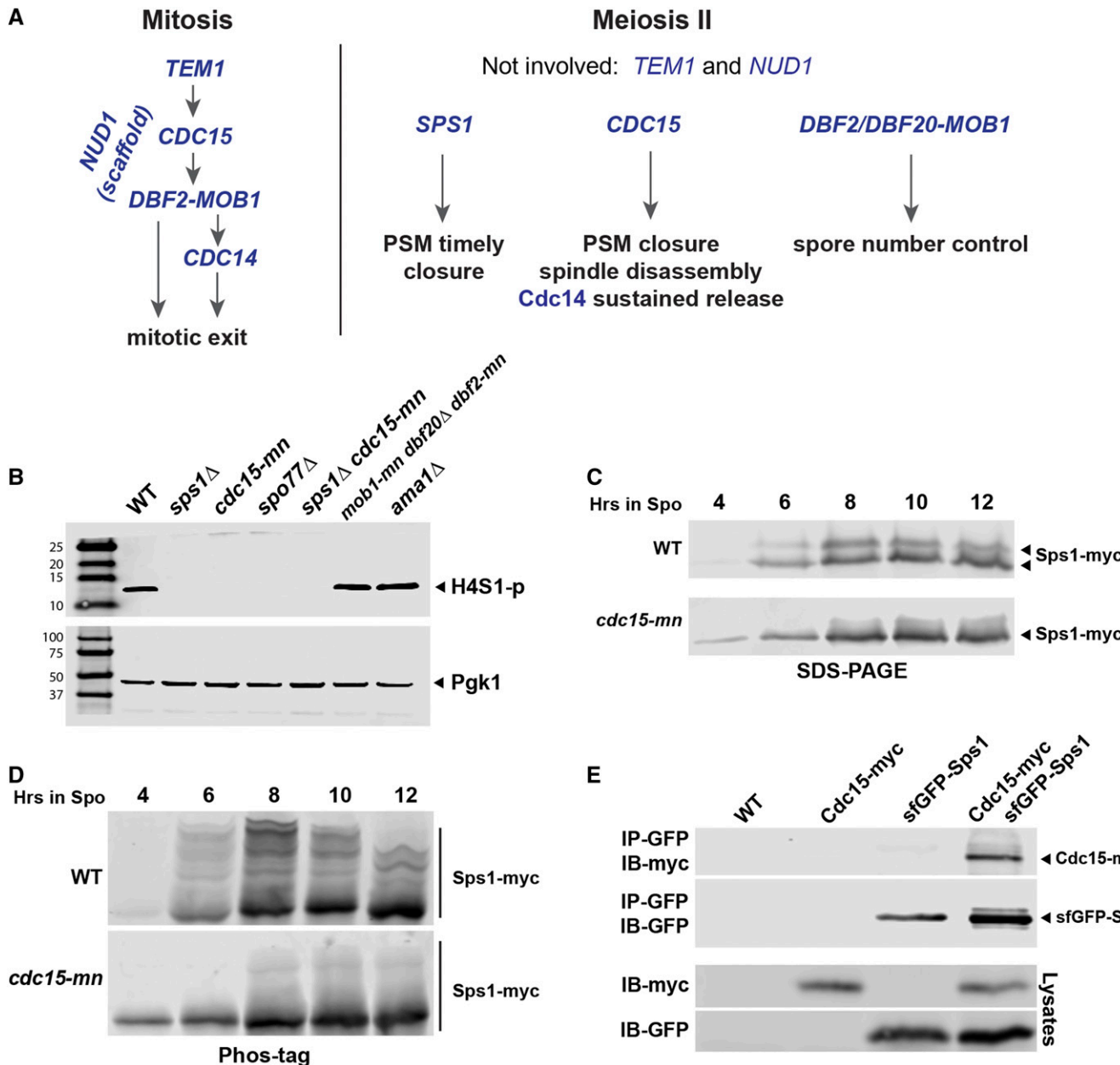


Figure 1 *CDC15* is required for *SPS1* phosphorylation. (A) Members of the mitotic exit network in mitosis and meiosis. See details and references in *Introduction*. (B) Screening for other genes deficient in histone phosphorylation. Cells lacking specific genes were induced to sporulate and collected at 8 hr after induction of sporulation. H4S1 phosphorylation was assayed by immunoblotting. *Pgk1* was used as a loading control and was from the top half of the same gel as was probed for histone phosphorylation. Protein marker sizes are shown to the left of the gel. Lysates were from wild-type (LH902), *sps1* (LH966), *cdc15* (LH1066), *spo77* (LH1010), *sps1 cdc15* (LH1067), *mob1 dbf2 dbf20* (LH1068), and *ama1* (LH1014). (C) *Sps1-13myc* was assayed on an SDS-PAGE gel using lysates from wild-type (LH875) and *cdc15-mn* (LH1069) cells that were collected at the indicated times after induction of sporulation, and probed with an anti-myc antibody. (D) *Sps1-13myc* was assayed using a Phos-tag gel using lysates from the same samples collected for (C). (E) *Cdc15* and *Sps1* form a complex. Immunoprecipitation experiments were carried out using lysates from wild-type (LH902), *Cdc15-myc* (LH1070), *sfGFP-Sps1* (LH986), and *Cdc15-myc sfGFP-Sps1* (LH1071). *Sps1* was immunoprecipitated using GFP-Trap beads. Immunoblots were probed with either anti-GFP antibody or anti-myc antibody. Note that all immunoblots have been run more than once with biological replicates, and all show the same results. WT, wild type.

mutant cells to wild type (Figure 3B). The observed delay in prospore membrane closure is not due to a delay in prospore membrane initiation, as *cdc15-mn* cells, like *sps1Δ* mutants (Paulissen *et al.* 2016), showed an onset of prospore membrane biogenesis similar to wild type.

SPS1 acts to regulate timely prospore membrane closure in a pathway in parallel to *AMA1*, as cells lacking *SPS1* or *AMA1* have partial defects in prospore membrane closure that is exacerbated in the double mutant (Paulissen *et al.* 2016). We tested whether *CDC15* also acts in parallel to

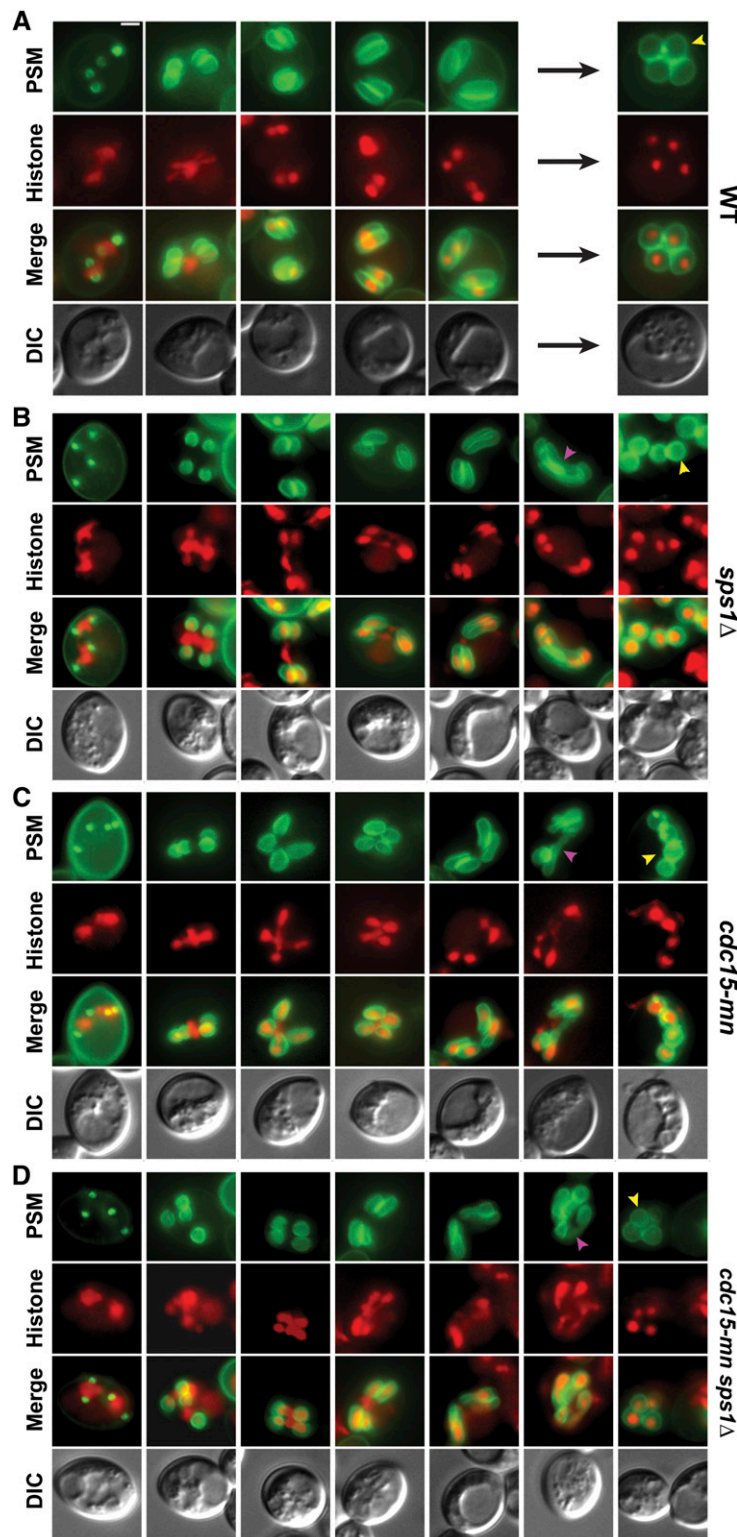
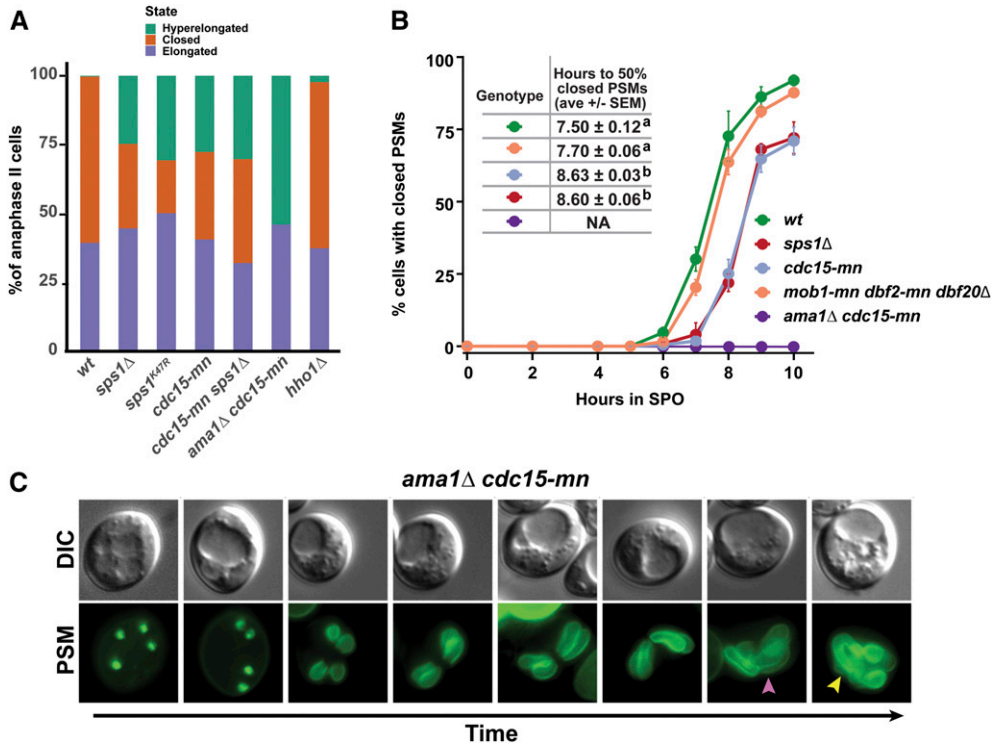


Figure 2 *CDC15* is required for proper prospore membrane development. Cells are of the following genotypes: (A) wild type (LH917), (B) *sps1Δ* (LH1047), (C) *cdc15-mn* (LH1073), and (D) *cdc15-mn* *sps1Δ* (LH1074). Prospore membranes are labeled in green, using the plasmids pRS426-G20 [wild type and *sps1Δ*] or pRS426-E20 [*cdc15-mn* and *sps1Δ cdc15-mn*]. Histones are labeled in red, using genetically integrated *HTB2-mCherry* fusion protein. Developmental stages are shown from early (left) to late (right). Pink arrowheads point to examples of hyperelongated prospore membranes. Yellow arrowheads point to examples of rounded prospore membranes. Images were captured using a wide-field microscope. WT, wild type.

AMA1 and examined doubly mutant *cdc15-mn ama1Δ* cells. We found that *cdc15-mn ama1Δ* cells form rounded prospore membranes at <0.1% frequency (Figure 3B), a much stronger defect than either *cdc15-mn* (Figure 3B) or *ama1Δ* cells alone (~30%; Diamond *et al.* 2009; Paulissen *et al.* 2016).

These *cdc15-mn ama1Δ* double mutant cells form prospore membranes that are hyperelongated (Figure 3A) and become highly invaginated, filling the cytoplasmic space of the mother cell and only rarely rounding up and closing (Figure 3C), similar to that seen in the *sps1Δ ama1Δ* double mutant



replicates per strain. Prospore membranes were visualized using pRS426-E20, except for one biological replicate of wild-type and *sps1* Δ strains, which used pRS426-G20. For 50% PSM closing, superscripts denote statistically distinct groups. (C) *ama1* Δ *cdc15-mn* (LH1076) mutants produce hyperelongated prospore membranes that do not close. Prospore membranes are labeled in green using the plasmid pRS426-E20. Prospore membranes are shown from early (left) to late (right) on the bottom row, with a corresponding DIC picture of the cell on top. Pink and yellow arrowheads point to examples of hyperelongated prospore membranes. Images were captured using a wide-field microscope. WT, wild type.

(Paulissen *et al.* 2016). These results taken together show that *CDC15* regulates timely prospore membrane closure, acting in the same pathway as *SPS1* and in parallel to *AMA1*.

SPS1 has a meiosis II spindle disassembly defect similar to *CDC15*

Cells lacking *CDC15* have been previously shown to have a meiosis II spindle disassembly defect (Pablo-Hernando *et al.* 2007; Attner and Amon 2012). Since *SPS1* and *CDC15* share prospore membrane phenotypes, we examined whether *SPS1* played a role in meiotic spindle disassembly.

We examined spindles in live wild-type, *sps1* Δ , and *cdc15-mn* sporulating cells using a functional GFP^{ENVY} tagged version of *TUB1* (α -tubulin) integrated at the *TUB1* locus, such that it retains the *TUB1* 3'UTR (Markus *et al.* 2015). Spindles in wild-type cells elongated and then disassembled during meiosis I and II, eventually forming small spindles in the newly created spores (Figure 4A). *cdc15-mn* cells failed to disassemble meiosis II spindles, with late anaphase II spindles becoming extended and ultimately fragmenting within the cell (Figure 4B), consistent with previous observations (Pablo-Hernando *et al.* 2007; Attner and Amon 2012).

sps1 Δ mutant cells had microtubule morphologies that were indistinguishable from that of the *cdc15-mn* mutant (Figure 4C), including the frequent occurrence of elongated, fragmented, and supernumerary microtubules late in anaphase II

(arrows in Figure 4C). When we examine the meiotic spindles in the *sps1* Δ *cdc15-mn* double mutant, we see that the microtubule morphology phenotype was indistinguishable to that of the single mutants (Figure 4D). We see the same microtubule morphology defects when we visualize microtubules using immunostaining in fixed sporulating cells (Figure S3).

We quantitated the spindle disassembly phenotype by counting the number of spindle fragments found in postanaphase II cells, and find that *cdc15-mn*, *sps1* Δ , and *cdc15-mn sps1* Δ cells are all statistically distinct from wild type (Figure 4F). These results are consistent with *SPS1* and *CDC15* acting in the same pathway for meiotic exit, which involves both meiotic spindle disassembly and cytokinesis, the latter accomplished via prospore membrane closure during yeast meiosis.

SPS1 kinase activity is required for its role in prospore membrane closure and spindle disassembly

To test whether the kinase activity of *Sps1* is required for its role in prospore membrane closure and spindle disassembly, we created *sps1* $K47R$, a genetically integrated *sps1* kinase dead allele that replaces a conserved lysine in the catalytic domain with arginine. We see that *sps1* $K47R$ cells have hyperelongated prospore membranes (Figure 3A), and have a spindle disassembly defect that produces microtubule morphologies similar to that seen in the *sps1* Δ and *cdc15-mn* cells (Figure 4E).

Figure 3 *CDC15* and *SPS1* are required for prospore membrane morphology and timely prospore membrane closure and act in parallel to *AMA1*. (A) Quantitation of prospore membrane morphology in wild-type (LH1081), *sps1* Δ (LH1089), *sps1* $K47R$ (LH1108), *cdc15-mn* (LH1073), *cdc15-mn sps1* Δ (LH1074), *ama1* Δ *cdc15-mn* (LH1076), and *hho1* Δ (LH1109). Cells scored blind for prospore membrane (PSM) morphology. At least 200 cells were counted per culture, in at least three biological replicates per strain. Chi-square analysis followed by pairwise Fisher's exact test (Bonferroni-corrected for multiple comparisons) showed that the percent of hyperelongated prospore membranes seen in wild type is significantly different from all other examined strains, except for *hho1* Δ ($P < 0.01$). (B) Quantitation of PSM closure in wild-type (LH1071 or LH1081), *sps1* Δ (LH1047 or LH1089), *cdc15-mn* (LH1073), *mob1-mn dbf2-mn dbf20A* (LH1082), and *ama1* Δ *cdc15-mn* (LH1075). At least 100 cells were counted per time point, for each genotype, with at least three biological

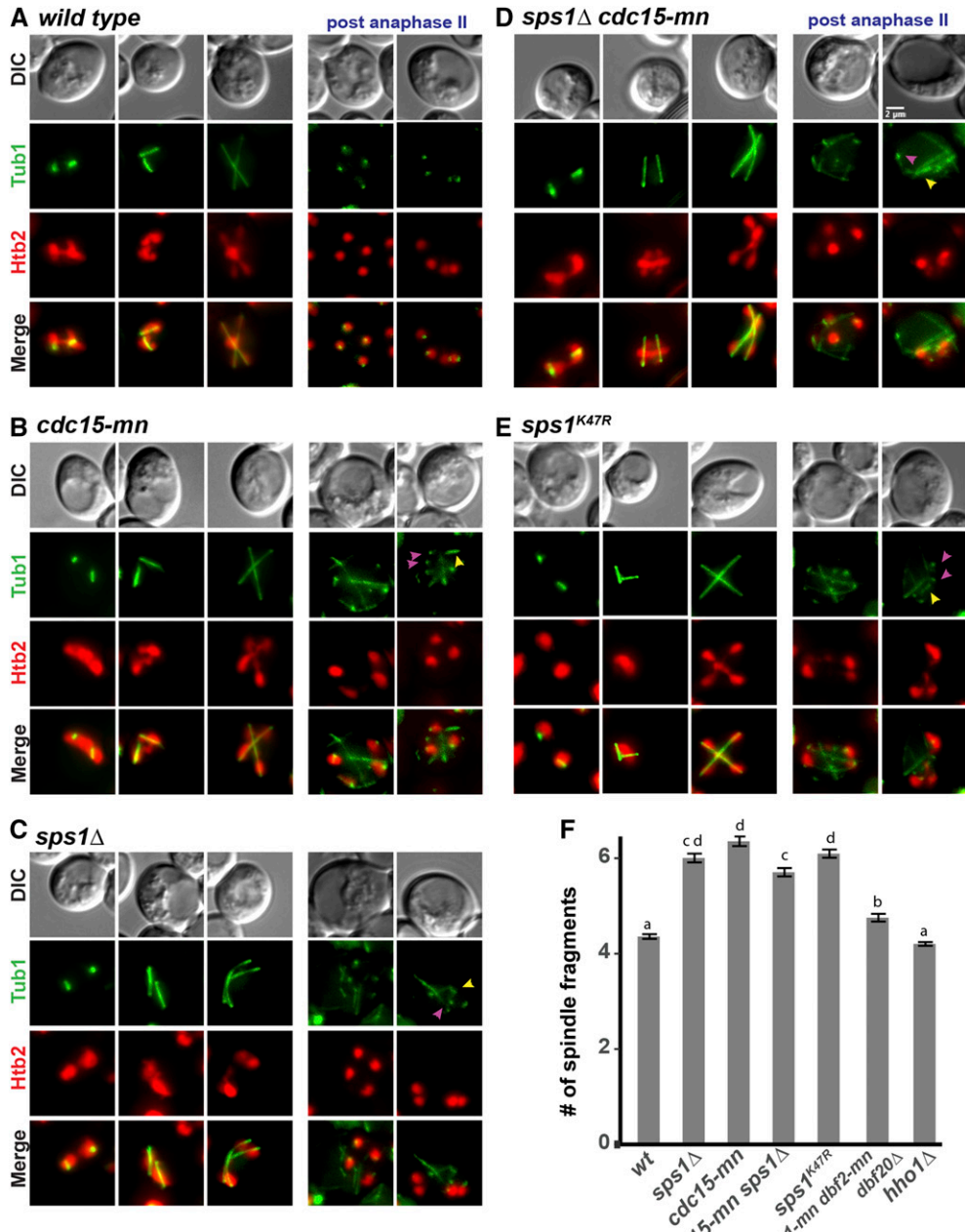


Figure 4 *SPS1* plays a role in spindle disassembly. Microtubules were visualized in green using *GFP^{ENVY}-TUB1*. Histones, in red, are visualized using *HTB2-mCherry*. Cells at different time points in meiosis, arrayed from early (left) to late (right), with two representative images of postanaphase II microtubule phenotypes shown for the strains. Images were captured using a wide-field microscope. Cells are of the following genotypes: (A) wild type (LH1095), (B) *cdc15-mn* (LH1096), (C) *sps1*^Δ (LH1097), (D) *sps1*^Δ *cdc15-mn* (LH1098), and (E) *sps1*^{K47R} (LH1102). Arrowheads point to examples of fragmented (yellow) and supernumerary (pink) microtubules. (F) Quantitation of the number of spindles in post-anaphase II cells. Three biological replicates were counted for each genotype, for a total of at least 150 cells per genotype. Error bars show the standard error of the mean. One way ANOVA [$F(6, 1127) = 131.03, P < 0.0001$], followed by Tukey Honest Significant Difference *post hoc* test ($\alpha = 0.01$); letters denote statistically distinct groups. WT, wild type.

When we quantitate the number of spindle fragments in *sps1*^{K47R} cells, we see that *cdc15-mn*, *sps1*^Δ, and *sps1*^{K47R} are not statistically distinct (Figure 4F). These results are consistent with the kinase activity of *Sps1* being required for timely prospore membrane closure and spindle disassembly.

Cdc14-sustained release in anaphase II requires SPS1

During mitosis, the MEN, a signal transduction network that utilizes *Cdc14* activation of *Dbf2-Mob1* NDR kinase complex (Rock *et al.* 2013), promotes the release of the *Cdc14* phosphatase from the nucleolus to inactivate mitotic CDK activity and promote exit from mitosis (Visintin *et al.* 1998; Shou *et al.* 1999; Mohl *et al.* 2009; Manzoni *et al.* 2010). In meiosis,

MEN is predominately active in meiosis II, with *Dbf20* as the major NDR kinase in meiosis, although *Dbf2* also plays a role (Attner and Amon 2012; Renicke *et al.* 2017).

During meiosis, *CDC14* acts in both meiosis I and meiosis II (Buonomo *et al.* 2003; Marston *et al.* 2003; Kamieniecki *et al.* 2005; Villoria *et al.* 2017; Fox *et al.* 2017). In meiosis, *Cdc14* is released from the nucleolus before anaphase I spindle elongation, then reappears in the nucleolus at the start of meiosis II, and is released again just before anaphase II (Bizzari and Marston 2011; Kerr *et al.* 2011); the initial release of *Cdc14* in meiosis requires the FEAR network and not the MEN (Buonomo *et al.* 2003; Marston *et al.* 2003; Kamieniecki *et al.* 2005; Pablo-Hernando *et al.* 2007). However, *CDC15* is required

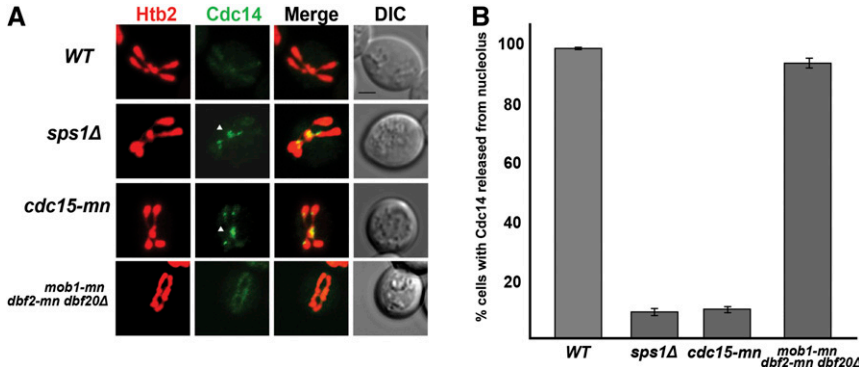


Figure 5 The sustained release of Cdc14 requires *SPS1* and *CDC15*, but not *DBF2* *DBF20* *MOB1*. (A) The Cdc14-GFP^{Env} fusion protein was visualized in wild-type (LH1077), *sps1Δ* (LH1078), *cdc15-mn* (LH1079), and *mob1-mn dbf2-mn dbf20Δ* (LH1080) cells. Representative images are shown from these strains. Histones are visualized using a genetically integrated *Htb2-mCherry*. Images were captured using a confocal microscope. White arrowhead points to nucleolar-localized Cdc14. Bar, 2 μ m. (B) Quantitation of cells in anaphase II (as determined by *Htb2-mCherry* localization) with Cdc14 released from the nucleolus. Cells were sporulated in triplicate, with 100 anaphase II cells counted for each biological replicate for a total of 300 cells per strain. Error bars represent standard error of the mean. The wild-type and triple mutant (*mob1-mn dbf2-mn dbf20Δ*) strains, but not from one another, one-way ANOVA [$F(3,8)=860$, $P < 0.001$], followed by Tukey Honest Significant Difference *post hoc* test ($\alpha = 0.01$). WT, wild type.

for the sustained release of Cdc14 during anaphase II (Pablo-Hernando *et al.* 2007; Attner and Amon 2012).

We first reexamined Cdc14 release during anaphase II in wild-type cells, using a *CDC14-GFP^{Env}* allele. We see dynamic localization for Cdc14 (Figure 5), as previously described (Bizzari and Marston 2011), with Cdc14 being released from the nucleolus and into the nucleus and cytoplasm during anaphase II. We also see, as previously described (Pablo-Hernando *et al.* 2007), that Cdc14 release is not properly sustained in anaphase II in the *cdc15-mn* mutants.

Given the role of *CDC15*, we asked whether *SPS1* plays a role in Cdc14 anaphase II release, and find that Cdc14 release is not properly sustained in *sps1Δ* mutants, similar to that seen in *cdc15-mn* mutants (Figure 5). The kinase activity of Sps1 is required for Cdc14 release, as we see a similar defect in *sps1K47R* cells (Figure S4). We confirmed localization of the Cdc14 to the nucleolus in *sps1Δ* and *cdc15-mn* mutants using the nucleolar marker Nop56/Sik1 (Gautier *et al.* 1997; Figure S5); the localization of the nucleolus at the center of the tetrad until very late in anaphase II is consistent with previous reports (Fuchs and Loidl 2004).

Because the Dbf2-Mob1 NDR kinase complex acts in between *CDC15* and *CDC14* during mitosis, we examined the role of NDR kinase complex in Cdc14 release in anaphase II. To inactivate this complex, we created the *dbf2-mn* allele, which places the mitotically required *DBF2* gene under the control of the mitosis-specific *CLB2* promoter. To eliminate as much NDR kinase complex activity in meiosis as possible, we combined the *dbf2-mn* allele with the previously constructed *mob1-mn* and the *dbf20Δ* alleles (Attner and Amon 2012). We see that the *mob1-mn dbf2-mn dbf20Δ* triple mutant strain displayed wild-type histone phosphorylation defect, unlike *sps1Δ* or *cdc15-mn* (Figure 1B).

When we examined Cdc14 release in the *mob1-mn dbf2-mn dbf20Δ* triple mutant strain, we find that Cdc14 is properly released during anaphase II, similar to what is seen in wild-type cells and in contrast to what is seen in the *cdc15* and *sps1* mutant cells (Figure 5). Thus, in meiosis II, the NDR kinase complex, encoded by *MOB1 DBF2 DBF20*, does not act

downstream of *CDC15* to regulate Cdc14 release. Instead, our results are consistent with *SPS1* acting downstream of *CDC15* to regulate Cdc14-sustained release during anaphase II.

***CDC15* and *SPS1* do not act with the NDR kinase complex for spore number control**

The NDR kinase complex has been previously shown to play a role in spore number control, a process that determines the number of spores packaged during meiosis (Renicke *et al.* 2017). Spore number control regulates the number of spindle pole bodies that are competent for prospore membrane growth; this process depends on a spindle pole body modification that occurs based on the age of the spindle pole body and the nutrients available to sporulating cells (Davidow *et al.* 1980; Nickas *et al.* 2004; Taxis *et al.* 2005). Depletion of the NDR kinase complex results in fewer spores per ascus forming during sporulation, as seen when *MOB1 DBF2 DBF20* activity was reduced using a protein depletion system (Renicke *et al.* 2017). We see a similar result using our *mob1-mn dbf2-mn dbf20Δ* strain, as assayed by counting refractile spores formed (Figure S6) or by counting the number of prospore membranes formed as a proxy for the number of spores than can form within the ascus (Figure 6).

Because neither *cdc15-mn* nor *sps1Δ* cells form refractile spores, we assayed spore number control by counting the number of prospore membranes that are present in anaphase II, to determine how many spores could form within an ascus. We see most *sps1Δ* and *cdc15-mn* mutant cells will initiate four prospore membranes per ascus, similar to that seen in wild-type cells, and unlike that seen in the *mob1-mn dbf2-mn dbf20Δ* mutants. These results suggest that neither *sps1Δ* nor *cdc15-mn* act with the NDR kinase complex in spore number control.

The NDR kinase complex does not play a role in timely prospore membrane closure or spindle disassembly

Because we see that the *Mob1-Dbf2/20* NDR kinase complex appears to regulate distinct biological processes from the *Cdc15* and *Sps1* kinases, we examined prospore membrane morphology and timing of prospore membrane closure in the

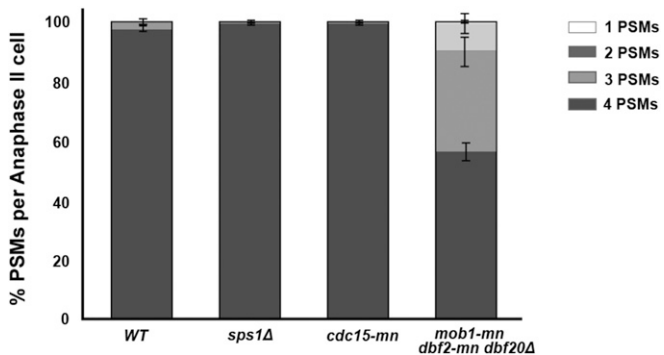


Figure 6 *SPS1* and *CDC15* are not required to regulate the number of prospore membranes formed. The number of prospore membranes (PSMs) formed per cell were counted in anaphase II cells, as assayed by visualizing histones using *Htb2-mCherry*. Prospore membranes were visualized using the plasmid pRS426-E20. Wild-type (LH1081), *sps1* Δ (LH1089), *cdc15-mn* (LH1073), and *mob1-mn dbf2-mn dbf20Δ* (LH1082) cells were used. Three biological replicates of 100 cells per replicate were counted, for a total of 300 cells per strain. Error bars represent standard error of the mean. The wild-type, *cdc15-mn*, and *sps1* Δ strains are significantly different from the triple mutant (*mob1-mn dbf2-mn dbf20Δ*) strain, but not from one another, using four PSMs as the variable for comparison; one-way ANOVA [$F(3,8) = 437$, $P < 0.001$], followed by Tukey Honest Significant Difference post hoc test ($\alpha = 0.01$). WT, wild type.

mob1-mn dbf2-mn dbf20Δ triple mutant. We find that the *mob1-mn dbf2-mn dbf20Δ* triple mutants do not form the characteristic hyperelongated prospore membranes seen in *sps1* Δ and *cdc15-mn* mutant cells, although aberrant prospore membrane size and nuclear capture defects were observed (Figure 7A). Furthermore, the *mob1-mn dbf2-mn dbf20Δ* mutant cells produced rounded prospore membranes with similar timing to wild-type cells, and do not exhibit the delay seen in *cdc15-mn* or *sps1* Δ mutant cells (Figure 3B).

Because we see a spindle disassembly defect in *sps1* and *cdc15-mn* mutant cells, we examined the spindle in the *mob1-mn dbf2-mn dbf20Δ* cells. *mob1-mn dbf2-mn dbf20Δ* triple mutant cells do not produce the elongated, fragmented, and supernumerary microtubules late in anaphase II that are seen in the *sps1* Δ , *cdc15-mn*, and *sps1* Δ *cdc15-mn* double mutant cells. Instead, in late meiosis II, spindles in the *mob1-mn dbf2-mn dbf20Δ* cells appear to be disassembled into shorter punctate pieces (Figure 7B), which is distinct from the fragmented microtubules seen in *sps1* Δ , *cdc15-mn*, and *sps1* Δ *cdc15-mn* late in anaphase II. When we quantitate the number of spindle fragments found in postanaphase II cells, we see that the number of fragments found in *mob1-mn dbf2-mn dbf20Δ* cells is statistically distinct from *cdc15-mn*, *sps1* Δ , *sps1* K47R , and *cdc15-mn sps1* Δ cells (Figure 4F). Thus, the NDR kinase complex does not appear to play the same role in timely prospore membrane closure or spindle disassembly as *SPS1* and *CDC15*.

The linker histone encoded by *HHO1* is not required for prospore membrane morphology, spindle disassembly, or *Cdc14*-sustained release

Because *CDC15* and *SPS1* affect histone H4 phosphorylation in meiosis II, and since H4 phosphorylation promotes chromatin

compaction in meiosis (Krishnamoorthy *et al.* 2006), we asked whether the meiosis II exit defects were an indirect effect of a general problem with chromatin. *HHO1* encodes a linker histone important for chromatin compaction during sporulation, but is not essential for viability; *Hho1* protein accumulates around the time of H4S1 phosphorylation (Bryant *et al.* 2012). We examined *hho1* Δ cells during sporulation and found that they do not make hyperelongated prospore membranes (Figures 3A and 8A), do not have a spindle disassembly defect (Figure 8B), are not statistically distinct from wild-type cells for the number of microtubules in postanaphase II cells (Figure 4F), and are not statistically distinct from wild-type cells for the number of cells that have released *Cdc14* from the nucleolus in anaphase II cells (Figure S4). Taken together, these data are consistent with a specific function for *SPS1* and *CDC15* in exit from meiosis II that is independent of their role in histone regulation.

Discussion

Our studies demonstrate that during meiosis, timely prospore membrane closure, meiosis II spindle disassembly, and sustained release of *Cdc14* at anaphase II are regulated by *SPS1* and *CDC15*, while the *Mob1-Dbf2/20* complex plays a separate role in meiosis regulating spore number control. These results suggest that for exit from meiosis II, the MEN is rewired, such that *Sps1* replaces the NDR kinase complex and acts downstream of the *Cdc15* kinase (Figure 8C).

SPS1 acts with *CDC15* to regulate exit from meiosis II

We describe two previously unknown roles for *SPS1* in the completion of meiosis: timely spindle disassembly and *Cdc14* sustained release. Prior to this study, the involvement of *SPS1* in sporulation was thought to be for spore morphogenesis (Friesen *et al.* 1994; Iwamoto *et al.* 2005), and, more specifically, for timely prospore membrane closure (Paulissen *et al.* 2016). Furthermore, *sps1* Δ and *cdc15-mn* mutants have identical phenotypes, as we describe a role for *CDC15* in timely prospore membrane closure. Since we see that *Cdc15* is needed for *Sps1* phosphorylation, these results are consistent with a model where *Sps1* acts downstream of *Cdc15* for exit from meiosis II (see model in Figure 8C).

Here, we show that the kinase activity of *Sps1* is needed for the completion of meiosis II. However, a better understanding of the mechanism underlying how this pathway leads to the exit of meiosis II will require identification of downstream targets. In mitosis, although the phosphorylation of many CDK targets are reversed by *Cdc14* upon mitotic exit, some downstream targets important for cytokinesis are directly phosphorylated by the *Dbf2* kinase (Meitinger *et al.* 2011, Oh *et al.* 2012). For meiosis, it is unknown whether *Cdc14* is phosphorylated by *Sps1*, whether all targets downstream of *CDC15* and *SPS1* are directly regulated by the *Cdc14* phosphatase, or whether *Sps1* may directly phosphorylate downstream targets as well. It is likely that *Sps1* plays some direct role, as previous studies have demonstrated that although

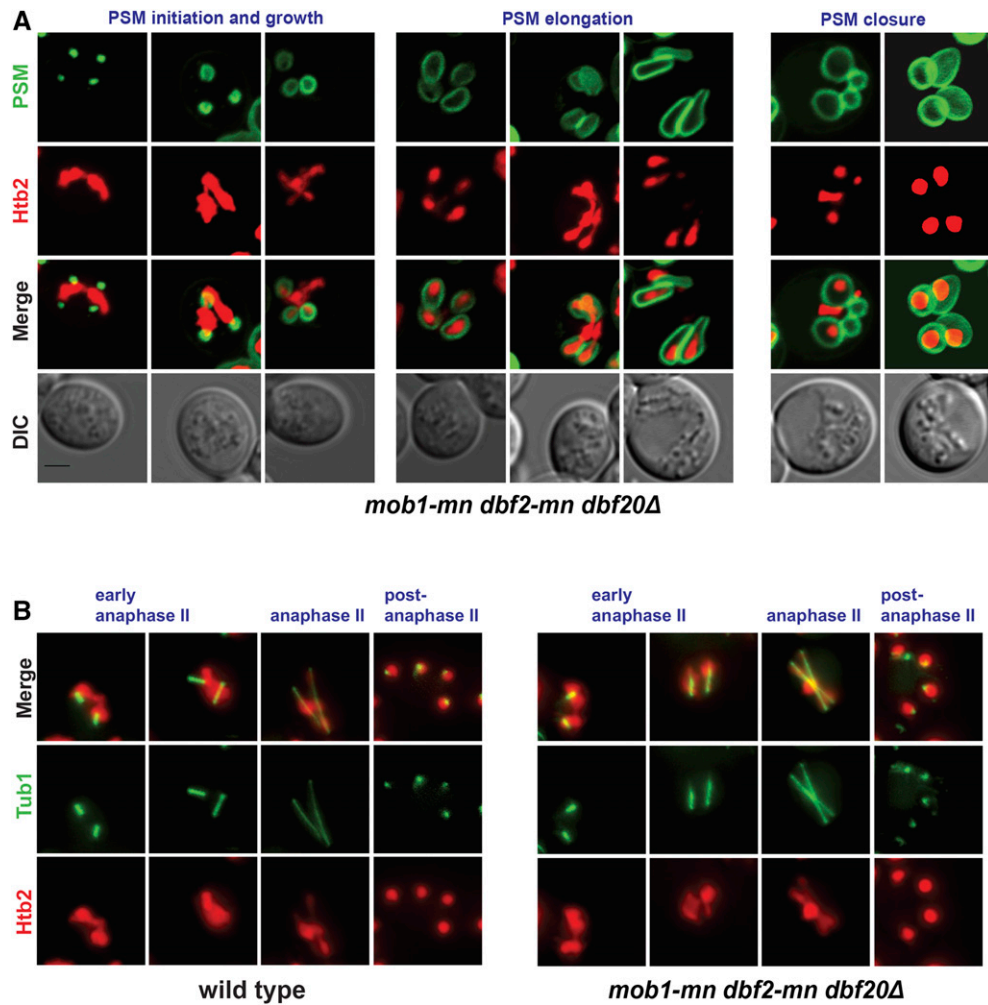


Figure 7 *DBF2 DBF20 MOB1* prospore membrane and spindle morphologies. (A) *mob1-mn dbf2-mn dbf20Δ* (LH1082) cells do not form hyperelongated prospore membranes (PSMs). Prospore membranes are labeled in green, using the plasmid pRS426-E20. Histones are visualized using *HTB2-mCherry*. Bar, 2 μ m. See quantitation in Figure 3A. (B) *DBF2 DBF20 MOB1* are not required for spindle disassembly. Microtubules were visualized in green using *GFP^{ENVY}-TUB1* in wild-type (LH1095) and *mob1-mn dbf2-mn dbf20Δ* (LH1099) cells. Histones, in red, are visualized using *HTB2-mCherry*. Cells at different time points in meiosis, arrayed from early (left) to late (right). Images were captured using a wide-field microscope. See quantitation in Figure 4F.

CDC15 is required for sustained *Cdc14* release, *CDC14* does not appear to play a role in meiosis II spindle disassembly or prospore membrane morphology (Pablo-Hernando *et al.* 2007; Argüello-Miranda *et al.* 2017). These studies depleted *CDC14* activity using either a *cdc14-ΔNES* allele, which deleted the *Cdc14* nuclear export signal at residues 359–367 (Pablo Hernando *et al.* 2007), or the *cdc14-3* temperature-sensitive allele (Argüello-Miranda *et al.* 2017). The role of *SPS1* in prospore membrane closure is likely to be *CDC14* independent, as *SPS1* is required for the phosphorylation and reduced stability of *Ssp1* (Paulissen *et al.* 2016), a protein localized to the leading edge of the growing prospore membrane that must be removed and degraded for this process to occur (Maier *et al.* 2007).

We find that *CDC15* and *SPS1* act in parallel to *AMA1*, which encodes a meiosis-specific activator of the anaphase promoting complex (APC/C) (Cooper *et al.* 2000). Previous studies have examined a hyperactive *ama1* allele (*ama1-m8*, which lacks eight consensus *Cdc28* phosphorylation sites in *Ama1*) in combination with *cdc15-mn*, and found a significant increase in prospore membrane closure in the double mutant (Diamond *et al.* 2009), consistent with our findings here. Interestingly,

AMA1 has also been linked to both spindle disassembly and prospore membrane closure. For meiosis II spindle disassembly, *AMA1* acts downstream of *HRR25*-encoded casein kinase 1 (Argüello-Miranda *et al.* 2017). *AMA1* regulates prospore membrane closure (Diamond *et al.* 2009; Paulissen *et al.* 2016) and affects the stability of *Ssp1*, localized at the leading edge of the prospore membrane (Diamond *et al.* 2009).

The combination of both meiosis II spindle disassembly and prospore membrane closure defects for *cdc15*, *spc1*, and *ama1* mutants raises the question of whether the prospore membrane closure defect seen in these mutants is a consequence of the stable meiosis II spindles, which are in the way and thus prevent the membrane fusion event required to close the membrane. Whether prospore membrane closure and spindle disassembly are coordinated by the regulation of a common target of both these pathways, or whether these two events are regulated via distinct targets, remains to be determined.

Cdc15 and the NDR/LATS kinase complex play distinct roles in meiosis

Our studies demonstrate that in meiosis II, cells appear to utilize *CDC15* and *MOB1-DBF2/20* for distinct roles, unlike in

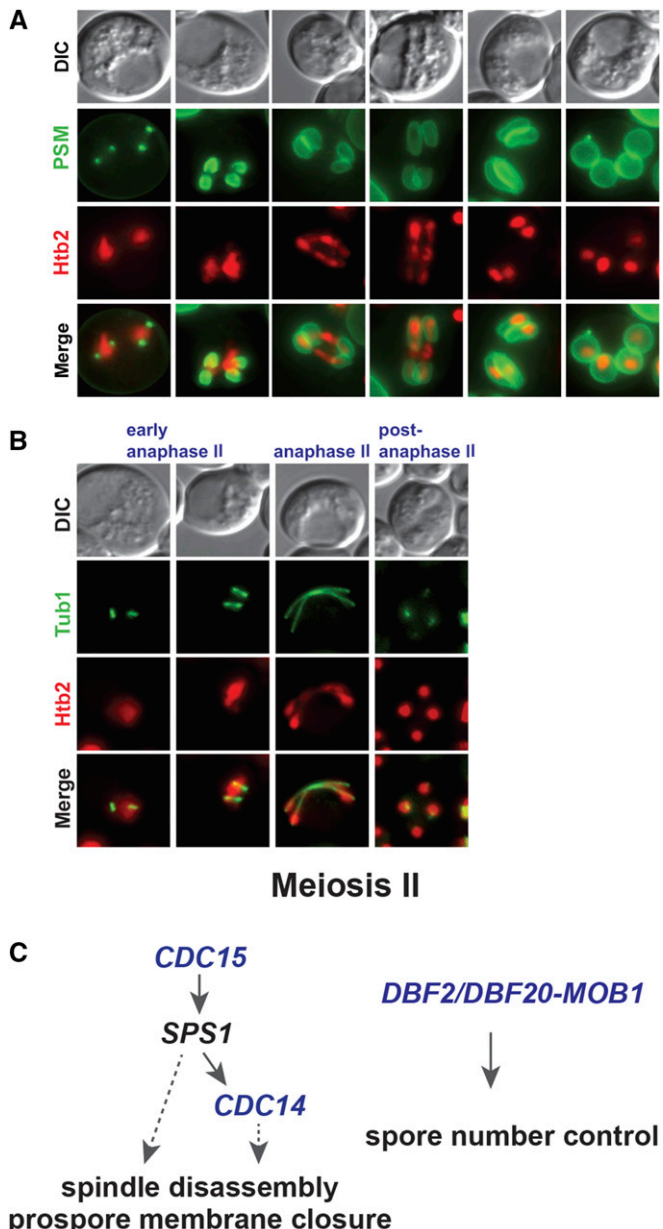


Figure 8 *HHO1* is not required for proper prospore membrane morphology or for spindle disassembly. (A) *hho1Δ* (LH1109) cells do not form hyperelongated prospore membranes (PSM). Prospore membranes are labeled in green using the plasmid pRS426-E20. Histones are visualized using *HTB2-mCherry*. See quantitation in Figure 3A. (B) *HHO1* is not required for spindle disassembly. Microtubules were visualized in green, using *GFPENVY-TUB1* in *hho1Δ* (LH1103) cells. Histones, in red, are visualized using *HTB2-mCherry*. Cells at different time points in meiosis, arrayed from early (left) to late (right). Images were captured using a wide-field microscope. See quantitation in Figure 4F. (C) Model depicting the relationship between mitotic exit members in mitosis and meiosis. See discussion in text.

mitosis, where *Cdc15* activates a conserved *Mob1-NDR* kinase signaling system, as seen in typical Hippo signaling (Hergovich and Hemmings 2012; Weiss 2012). In meiosis II, it appears that *MOB1-DBF2/20* is important for spore number control (Reincke *et al.* 2017), in which neither *CDC15* nor

SPS1 play a role, as assayed by the number of prospore membranes formed.

Previous work described a role for *CDC15* in spore number control, with *cdc15*-depleted mutants forming more meiotic plaques on the spindle pole bodies when sporulated in low-acetate conditions, compared to wild-type cells and the *mob1 dbf2 dbf20* triple mutant (Reincke *et al.* 2017). We do not see a difference between *cdc15-mn* and wild-type cells in spore number control when using a direct assay of counting the number of prospore membranes formed in 1% acetate (Figure 6). Under our sporulation conditions, it may not be possible to see the *CDC15* effect, as most wild-type cells produce four prospore membranes (although we can see the effect of the NDR/LATS kinase complex on spore number control under these conditions; Figure S3). Importantly, the previous study found that the *mob1 dbf2 dbf20*-depleted triple mutant had a distinct phenotype from *cdc15*-depleted mutants in spore number control (Reincke *et al.* 2017), consistent with our findings that *Cdc15* and the NDR/LATS kinase complex play distinct roles in meiosis (Figure 8B).

Previous studies have shown that *Dbf20* kinase activity depends on *CDC15* in meiosis II, and the interaction of *Dbf20* and *Mob1* is dependent on *CDC15* (Attner and Amon 2012). However, our phenotypic characterization is consistent with the exit from meiosis functions of *CDC15* not requiring *DBF2/20-MOB1*. As the dependence on *CDC15* for both *Dbf20* kinase activity and the *Dbf20-Mob1* interaction was demonstrated biochemically (Attner and Amon 2012), it is not known what biological function of *Dbf20-Mob1* in meiosis requires *CDC15*.

GCK kinase as an alternative member of the Hippo signaling pathway

We found that meiosis II employs a modified Hippo signaling module that utilizes *Sps1*, an *STE20* family GCKIII kinase (Slubowski *et al.* 2014). Modifications of the typical Hippo signaling module to include *STE20* family GCK kinases have been reported. For example, in fission yeast, Hippo signaling also involves the intervening GCK family kinase *Sid1*, which acts between the *Cdc7* Hippo-like kinase and the *Mob1/Sid2* NDR kinase for septation (referred to as the SIN pathway) (Guertin *et al.* 2000). For tracheal morphogenesis in *Drosophila*, the NDR kinase *Trc* is activated by Germinal center kinase III, a GCKIII kinase (Poon *et al.* 2018). Unlike these previously described cases of GCK use that involve a downstream NDR/LATS kinase, for budding yeast meiosis, it appears that there has been a separation of function between the Hippo-GCKIII module and the downstream *Mob1-Dbf2/20* NDR/LATS kinase, providing a distinct example of how Hippo signaling can act with GCK members. Thus, Hippo signaling pathways are evolutionarily plastic, utilizing Hippo-GCKIII, Hippo-GCKIII-NDR/LATS, or Hippo-NDR/LATS cascades, depending on the organism, tissue, or differentiation state of the cell.

Acknowledgments

We thank the Amon laboratory for strains, Yasuyuki Suda for assistance with strain construction, Matt Durant for

comments on the manuscript, and Angelika Amon for comments on an earlier version of this work. This work was funded by grants from the National Institutes of Health to L.S.H. (GM86805) and A.M.N. (GM072540), and a Sanofi-Genzyme/College of Science and Mathematics Dean's Doctoral Research Fellowship to S.M.P. and B.C.S. S.N.-T. was supported by a National Institutes of Health Initiative for Maximizing Student Development grant (GM076321).

Literature Cited

- Argüello-Miranda, O., I. Zagoriy, V. Mengoli, J. Rojas, K. Jonak *et al.*, 2017 Casein kinase 1 coordinates cohesin cleavage, gametogenesis, and exit from M phase in Meiosis II. *Dev. Cell* 40: 37–52. <https://doi.org/10.1016/j.devcel.2016.11.021>
- Attner, M. A., and A. Amon, 2012 Control of the mitotic exit network during meiosis. *Mol. Biol. Cell* 23: 3122–3132. <https://doi.org/10.1091/mbc.e12-03-0235>
- Bardin, A. J., and A. Amon, 2001 MEN and SIN: what's the difference? *Nat. Rev. Mol. Cell Biol.* 2: 815–826. <https://doi.org/10.1038/35099020>
- Bertazzi, D. T., B. Kurtulmus, and G. Pereira, 2011 The cortical protein Lte1 promotes mitotic exit by inhibiting the spindle position checkpoint kinase Kin4. *J. Cell Biol.* 193: 1033–1048. <https://doi.org/10.1083/jcb.201101056>
- Bizzari, F., and A. L. Marston, 2011 Cdc55 coordinates spindle assembly and chromosome disjunction during meiosis. *J. Cell Biol.* 193: 1213–1228. <https://doi.org/10.1083/jcb.201103076>
- Bryant, J. M., J. Govin, L. Zhang, G. Gonahue, B. F. Pugh, *et al.*, 2012 The linker histone plays a dual role during gametogenesis in *Saccharomyces cerevisiae*. *Mol. Cell. Biol.* 32: 2771–2783. <https://doi.org/10.1128/MCB.00282-12>
- Buonomo, S. B., K. P. Rabitsch, J. Fuchs, S. Gruber, M. Sullivan *et al.*, 2003 Division of the nucleolus and its release of *CDC14* during anaphase of meiosis I depends on separase, *SPO12*, and *SLK19*. *Dev. Cell* 4: 727–739. [https://doi.org/10.1016/S1534-5807\(03\)00129-1](https://doi.org/10.1016/S1534-5807(03)00129-1)
- Campbell, I. W., X. Zhou, and A. Amon, 2019 The mitotic exit network integrates temporal and spatial signals by distributing regulation across multiple components. *eLife* 8: e41139. <https://doi.org/10.7554/eLife.41139>
- Chan, L. Y., and A. Amon, 2010 Spindle position is coordinated with cell-cycle progression through establishment of mitotic exit-activating and -inhibitory zones. *Mol. Cell* 39: 444–454. <https://doi.org/10.1016/j.molcel.2010.07.032>
- Cooper, K. F., M. J. Mallory, D. B. Egeland, M. Jarnik, and R. Strich, 2000 Ama1p is a meiosis-specific regulator of the anaphase promoting complex/cyclosome in yeast. *Proc. Natl. Acad. Sci. USA* 97: 14548–14553. <https://doi.org/10.1073/pnas.250351297>
- D'Aquino, K. E., F. Monje-Casas, J. Paulson, V. Reiser, G. M. Charles *et al.*, 2005 The protein kinase Kin4 inhibits exit from mitosis in response to spindle position defects. *Mol. Cell* 19: 223–234. <https://doi.org/10.1016/j.molcel.2005.06.005>
- Davidow, L. S., L. Goetsch, and B. Byers, 1980 Preferential occurrence of nonsister spores in two-spored asci of *Saccharomyces cerevisiae*: evidence for regulation of spore-wall formation by the spindle pole body. *Genetics* 94: 581–595.
- Diamond, A. E., J. S. Park, I. Inoue, H. Tachikawa, and A. M. Neiman, 2009 The anaphase promoting complex targeting subunit Ama1 links meiotic exit to cytokinesis during sporulation in *Saccharomyces cerevisiae*. *Mol. Biol. Cell* 20: 134–145. <https://doi.org/10.1091/mbc.e08-06-0615>
- Falk, J. E., I. W. Campbell, K. Joyce, J. Whalen, A. Seshan *et al.*, 2016 *LTE1* promotes exit from mitosis by multiple mechanisms. *Mol. Biol. Cell* 27: 3991–4001. <https://doi.org/10.1091/mbc.E16-08-0563>
- Fox, C., J. Zou, J. Rappaport, and A. L. Marston, 2018 Cdc14 phosphatase directs centrosome re-duplication at the meiosis I to meiosis II transition in budding yeast. *Wellcome Open Res.* 2: 2. <https://doi.org/10.12688/wellcomeopenres.10507.2>
- Fuchs, J., and J. Loidl, 2004 Behaviour of nucleolus organizing regions (NORs) and nucleoli during mitotic and meiotic divisions in budding yeast. *Chromosome Res.* 12: 427–438. <https://doi.org/10.1023/B:CHRO.0000034726.05374.db>
- Friesen, H., R. Lunz, S. Doyle, and J. Segall, 1994 Mutation of the *SPS1*-encoded protein kinase of *Saccharomyces cerevisiae* leads to defects in transcription and morphology during spore formation. *Genes Dev.* 8: 2162–2175. <https://doi.org/10.1101/gad.8.18.2162>
- Gautier, T., T. Berges, D. Tollervé, and E. Hurt, 1997 Nucleolar KKE/D repeat proteins Nop56p and Nop58p interact with Nop1p and are required for ribosome biogenesis. *Mol. Cell. Biol.* 17: 7088–7098. <https://doi.org/10.1128/MCB.17.12.7088>
- Gordon, O., C. Taxis, P. J. Keller, A. Benjak, E. H. K. Stelzer *et al.*, 2006 Nud1p, the yeast homolog of Centriolin, regulates spindle pole body inheritance in meiosis. *EMBO J.* 25: 3856–3868. <https://doi.org/10.1038/sj.emboj.7601254>
- Gruneberg, U., K. Campbell, C. Simpson, J. Grindlay, and E. Schieber, 2000 Nud1p links astral microtubule organization and the control of exit from mitosis. *EMBO J.* 19: 6475–6488. <https://doi.org/10.1093/emboj/19.23.6475>
- Guertin, D. A., L. Chang, F. Irshad, K. L. Gould, and D. McCollum, 2000 The role of the sid1p kinase and cdc14p in regulating the onset of cytokinesis in fission yeast. *EMBO J.* 19: 1803–1815. <https://doi.org/10.1093/emboj/19.8.1803>
- Hergovich, A., and B. A. Hemmings, 2012 Hippo signaling in the G2/M cell cycle phase: lessons learned from the yeast MEN and SIN pathways. *Semin. Cell Dev. Biol.* 23: 794–802. <https://doi.org/10.1016/j.semcdb.2012.04.001>
- Huang, L. S., H. K. Doherty, and I. Herskowitz, 2005 The Smk1p MAP kinase negatively regulates Gsc2p, a 1,3-beta-glucan synthase, during spore wall morphogenesis in *Saccharomyces cerevisiae*. *Proc. Natl. Acad. Sci. USA* 102: 12431–12436. <https://doi.org/10.1073/pnas.0502324102>
- Iwamoto, M. A., S. R. Fairclough, S. A. Rudge, and J. Engebrecht, 2005 *Saccharomyces cerevisiae* Sps1p regulates trafficking of enzymes required for spore wall synthesis. *Eukaryot. Cell* 4: 536–544. <https://doi.org/10.1128/EC.4.3.536-544.2005>
- Jaspersen, S. L., and D. O. Morgan, 2000 Cdc14 activates cdc15 to promote mitotic exit in budding yeast. *Curr. Biol.* 10: 615–618. [https://doi.org/10.1016/S0960-9822\(00\)00491-7](https://doi.org/10.1016/S0960-9822(00)00491-7)
- Jones, M. H., J. M. Keck, C. C. Wong, T. Xu, J. R. Yates, 3rd *et al.*, 2011 Cell cycle phosphorylation of mitotic exit network (MEN) proteins. *Cell Cycle* 10: 3435–3440. <https://doi.org/10.4161/cc.10.20.17790>
- Juanes, M. A., and S. Piatti, 2016 The final cut: cell polarity meets cytokinesis at the bud neck in *S. cerevisiae*. *Cell. Mol. Life Sci.* 73: 3115–3136. <https://doi.org/10.1007/s0018-016-2220-3>
- Kamieniecki, R. J., L. Liu, and D. S. Dawon, 2005 FEAR but not MEN genes are required for exit from meiosis I. *Cell Cycle* 4: 1093–1098. <https://doi.org/10.4161/cc.4.8.1857>
- Kane, S. M., and R. Roth, 1974 Carbohydrate metabolism during ascospore development in yeast. *J. Bacteriol.* 118: 8–14. <https://doi.org/10.1128/JB.118.1.8-14.1974>
- Kerr, G. W., S. Sarkar, K. L. Tibbles, M. Petronczki, J. B. A. Millar, *et al.*, 2011 Meiotic nuclear divisions in budding yeast require PP2A (CDC55)-mediated antagonism of Net1 phosphorylation by Cdk. *J. Cell Biol.* 193: 1157–1166. <https://doi.org/10.1083/jcb.201103019>

- Kinoshita, E., E. Kinoshita-Kikuta, K. Takiyama, and T. Koike, 2006 Phosphate-binding tag, a new tool to visualize phosphorylated proteins. *Mol. Cell. Proteomics* 5: 749–757. <https://doi.org/10.1074/mcp.T500024-MCP200>
- Knop, M., and K. Strasser, 2000 Role of the spindle pole body of yeast in mediating assembly of the prospore membrane during meiosis. *EMBO J.* 19: 3657–3667. <https://doi.org/10.1093/emboj/19.14.3657>
- Krishnamoorthy, T., X. Chen, J. Govin, W. L. Cheung, J. Dorsey *et al.*, 2006 Phosphorylation of histone H4 Ser1 regulates sporulation in yeast and is conserved in fly and mouse spermatogenesis. *Genes Dev.* 20: 2580–2592. <https://doi.org/10.1101/gad.1457006>
- Lam, C., E. Santore, E. Lavoie, L. Needleman, N. Fiacco *et al.*, 2014 A visual screen of protein localization during sporulation identifies new components of prospore membrane-associated complexes in budding yeast. *Eukaryot. Cell* 13: 383–391. <https://doi.org/10.1128/EC.00333-13>
- Lee, B. H., and A. Amon, 2003 Role of Polo-like kinase *CDC5* in programming meiosis I chromosome segregation. *Science* 300: 482–486. <https://doi.org/10.1126/science.1081846>
- Lee, S., W. A. Lim, and K. S. Thorn, 2013 Improved blue, green, and red fluorescent protein tagging vectors for *S. cerevisiae*. *PLoS One* 8: e67902. <https://doi.org/10.1371/journal.pone.0067902>
- Longtine, M. S., A. McKenzie, D. J. Demarini, N. G. Shah, A. Wach *et al.*, 1998 Additional modules for versatile and economical PCR-based gene deletion and modification in *Saccharomyces cerevisiae*. *Yeast* 14: 953–961. [https://doi.org/10.1002/\(SICI\)1097-0061\(199807\)14:10<953::AID-YEA293>3.0.CO;2-U](https://doi.org/10.1002/(SICI)1097-0061(199807)14:10<953::AID-YEA293>3.0.CO;2-U)
- Luca, F. C., M. Mody, C. Kurischko, D. M. Roof, T. H. Giddings *et al.*, 2001 *Saccharomyces cerevisiae* *Mob1p* is required for cytokinesis and mitotic exit. *Mol. Cell. Biol.* 21: 6972–6983. <https://doi.org/10.1128/MCB.21.20.6972-6983.2001>
- Maekawa, H., C. Priest, J. Lechner, G. Pereira, and E. Schiebel, 2007 The yeast centrosome translates the positional information of the anaphase spindle into a cell cycle signal. *J. Cell Biol.* 179: 423–436. <https://doi.org/10.1083/jcb.200705197>
- Mah, A. S., J. Jang, and R. J. Deshaies, 2001 Protein kinase *Cdc15* activates the *Dbf2-Mob1* kinase complex. *Proc. Natl. Acad. Sci. USA* 98: 7325–7330. <https://doi.org/10.1073/pnas.141098998>
- Maier, P., N. Rathfelder, M. G. Finkbeiner, C. Taxis, M. Mazza *et al.*, 2007 Cytokinesis in yeast meiosis depends on the regulated removal of *Ssp1p* from the prospore membrane. *EMBO J.* 26: 1843–1852. <https://doi.org/10.1038/sj.emboj.7601621>
- Manzoni, R., F. Montani, C. Visintin, F. Caudron, A. Ciliberto *et al.*, 2010 Oscillations in *Cdc14* release and sequestration reveal a circuit underlying mitotic exit. *J. Cell Biol.* 190: 209–222. <https://doi.org/10.1083/jcb.201002026>
- Markus, S. M., S. Omer, K. Baranowski, and W.-L. Lee, 2015 Improved plasmids for fluorescent protein tagging of microtubules in *Saccharomyces cerevisiae*. *Traffic* 16: 773–786. <https://doi.org/10.1111/tra.12276>
- Marston, A. L., B. H. Lee, and A. Amon, 2003 The *Cdc14* phosphatase and the FEAR network control meiotic spindle disassembly and chromosome segregation. *Dev. Cell* 4: 711–726. [https://doi.org/10.1016/S1534-5807\(03\)00130-8](https://doi.org/10.1016/S1534-5807(03)00130-8)
- Meitinger, F., M. E. Boehm, A. Hoffmann, B. Hub, H. Zentgraf *et al.*, 2011 Phosphorylation-dependent regulation of the F-BAR protein *Hof1* during cytokinesis. *Genes Dev.* 25: 875–888. <https://doi.org/10.1101/gad.622411>
- Mohl, D. A., M. J. Huddleston, T. S. Collingwood, R. S. Annan, and R. J. Deshaies, 2009 *Dbf2-Mob1* drives relocation of protein phosphatase *Cdc14* to the cytoplasm during exit from mitosis. *J. Cell Biol.* 184: 527–539. <https://doi.org/10.1083/jcb.200812022>
- Moreno-Borchart, A. C., K. Strasser, M. G. Finkbeiner, A. Shevchenko, A. Shevchenko *et al.*, 2001 Prospore membrane formation linked to the leading edge protein (LEP) coat assembly. *EMBO J.* 20: 6946–6957. <https://doi.org/10.1093/embj/20.24.6946>
- Nakanishi, H., P. de los Santos, and A. M. Neiman, 2004 Positive and negative regulation of a SNARE protein by control of intracellular localization. *Mol. Biol. Cell* 15: 1802–1815. <https://doi.org/10.1091/mbc.e03-11-0798>
- Neiman, A. M., 2011 Sporulation in the budding yeast *Saccharomyces cerevisiae*. *Genetics* 189: 737–765. <https://doi.org/10.1534/genetics.111.127126>
- Neiman, A. M., L. Katz, and P. J. Brennwald, 2000 Identification of domains required for developmentally regulated SNARE function in *Saccharomyces cerevisiae*. *Genetics* 155: 1643–1655.
- Nickas, M. E., and A. M. Neiman, 2002 *Ady3p* links spindle pole body function to spore wall synthesis in *Saccharomyces cerevisiae*. *Genetics* 160: 1439–50. <https://www.ncbi.nlm.nih.gov/pmc/articles/PMC1462073/>
- Nickas, M. E., A. E. Diamond, M.-J. Yang, and A. M. Neiman, 2004 Regulation of spindle pole function by an intermediary metabolite. *Mol. Biol. Cell* 15: 2606–2616. <https://doi.org/10.1091/mbc.e04-02-0128>
- Oh, Y., K. J. Chang, P. Orlean, C. Wloka, R. Deshaies *et al.*, 2012 Mitotic exit kinase *Dbf2* directly phosphorylates chitin synthase *Chs2* to regulate cytokinesis in budding yeast. *Mol. Biol. Cell* 23: 2445–2456. <https://doi.org/10.1091/mbc.e12-01-0033>
- Pablo-Hernando, M. E., Y. Arnaiz-Pita, H. Nakanishi, D. Dawson, F. del Rey *et al.*, 2007 *Cdcc15* is required for spore morphogenesis independently of *Cdc14* in *Saccharomyces cerevisiae*. *Genetics* 177: 281–293. <https://doi.org/10.1534/genetics.107.076133>
- Paulissen, S. M., C. J. Slubowski, J. M. Roesner, and L. S. Huang, 2016 Timely closure of the prospore Membrane requires *SPS1* and *SPO77* in *Saccharomyces cerevisiae*. *Genetics* 204: 1203–1216. <https://doi.org/10.1534/genetics.115.183939>
- Pereira, G., and E. Schiebel, 2005 Kin4 kinase delays mitotic exit in response to spindle alignment defects. *Mol. Cell* 19: 209–221. <https://doi.org/10.1016/j.molcel.2005.05.030>
- Philips, J., and I. Herskowitz, 1998 Identification of *Kel1p*, a Kelch domain-containing protein involved in cell fusion and morphology in *Saccharomyces cerevisiae*. *J. Cell Biol.* 143: 375–389. <https://doi.org/10.1083/jcb.143.2.375>
- Poon, C. L. C., W. Liu, Y. Song, M. Gomez, Y. Kulaberoglu *et al.*, 2018 A hippo-like signaling pathway controls tracheal morphogenesis in *Drosophila melanogaster*. *Dev. Cell* 47: 564–575.e5. <https://doi.org/10.1016/j.devcel.2018.09.024>
- Rabitsch, K. P., A. Toth, M. Galova, A. Schleiffer, G. Schaffner *et al.*, 2001 A screen for genes required for meiosis and spore formation based on whole-genome expression. *Curr. Biol.* 11: 1001–1009. [https://doi.org/10.1016/S0960-9822\(01\)00274-3](https://doi.org/10.1016/S0960-9822(01)00274-3)
- Renicke, C., A.-K. Allman, A. P. Lutz, T. Heimerl, and C. Taxis, 2017 The Mitotic Exit Network regulates spindle pole body selection during sporulation of *Saccharomyces cerevisiae*. *Genetics* 206: 919–937. <https://doi.org/10.1534/genetics.116.194522>
- Rock, J. M., and A. Amon, 2011 *Cdc15* integrates *Tem1* GTPase-mediated spatial signals with Polo kinase-mediated temporal cues to activate mitotic exit. *Genes Dev.* 25: 1943–1954. <https://doi.org/10.1101/gad.17257711>
- Rock, J. M., D. Lim, L. Stach, R. W. Ogrodniewicz, J. M. Keck *et al.*, 2013 Activation of the yeast Hippo pathway by phosphorylation-dependent assembly of signaling complexes. *Science* 340: 871–875. <https://doi.org/10.1126/science.1235822>
- Rose, M. D., and G. R. Fink, 1990 *Methods in Yeast Genetics*, Cold Spring Harbor Laboratory Press, Cold Spring Harbor, NY.
- Schindelin, J., I. Arganda-Carreras, E. Frise, V. Kaynig, M. Longair *et al.*, 2012 Fiji: an open-source platform for biological-image analysis. *Nat. Methods* 9: 676–682. <https://doi.org/10.1038/nmeth.2019>

- Schneider, C. A., W. S. Rasband, and K. W. Eliceiri, 2012 NIH Image to ImageJ: 25 years of image analysis. *Nat. Methods* 9: 671–675. <https://doi.org/10.1038/nmeth.2089>
- Schweitzer, B., and P. Philippse, 1991 *CDC15*, an essential cell cycle gene in *Saccharomyces cerevisiae*, encodes a protein kinase domain. *Yeast* 7: 265–273. <https://doi.org/10.1002/yea.320070308>
- Shou, W., J. H. Seol, A. Shevchenko, C. Baskerville, D. Moazed *et al.*, 1999 Exit from mitosis is triggered by Tem1-dependent release of the protein phosphatase Cdc14 from nucleolar RENT complex. *Cell* 97: 233–244. [https://doi.org/10.1016/S0092-8674\(00\)80733-3](https://doi.org/10.1016/S0092-8674(00)80733-3)
- Slubowski, C. J., S. M. Paulissen, and L. S. Huang, 2014 The GCKIII kinase Sps1 and the 14-3-3 isoforms, Bmh1 and Bmh2, cooperate to ensure proper sporulation in *Saccharomyces cerevisiae*. *PLoS One* 9: e113528. <https://doi.org/10.1371/journal.pone.0113528>
- Slubowski, C. J., A. D. Funk, J. M. Roesner, S. M. Paulissen, and L. S. Huang, 2015 Plasmids for C-terminal tagging in *Saccharomyces cerevisiae* that contain improved GFP proteins, Envy and Ivy. *Yeast* 32: 379–387. <https://doi.org/10.1002/yea.3065>
- Stegmeier, F., and A. Amon, 2004 Closing mitosis: the functions of the Cdc14 phosphatase and its regulation. *Annu. Rev. Genet.* 38: 203–232. <https://doi.org/10.1146/annurev.genet.38.072902.093051>
- Taxis, C., P. Keller, Z. Kavagiou, L. J. Jensen, J. Colombelli *et al.*, 2005 Spore number control and breeding in *Saccharomyces cerevisiae*: a key role for a self-organizing system. *J. Cell Biol.* 171: 627–640. <https://doi.org/10.1083/jcb.200507168>
- Villoria, M. T., F. Ramos, E. Duenas, P. Faull, P. Rodriguez Cutillas, *et al.*, 2017 Stabilization of the metaphase spindle by Cdc14 is required for recombinational DNA repair. *EMBO J.* 36: 79–101. <https://doi.org/10.1525/embj.201593540>
- Visintin, R., and A. Amon, 2001 Regulation of the mitotic exit protein kinases Cdc15 and Dbf2. *Mol. Biol. Cell* 12: 2961–2974. <https://doi.org/10.1091/mbc.12.10.2961>
- Visintin, R., K. Craig, E. S. Hwang, S. Prinz, M. Tyers *et al.*, 1998 The phosphatase Cdc14 triggers mitotic exit by reversal of Cdk-dependent phosphorylation. *Mol. Cell* 2: 709–718. [https://doi.org/10.1016/S1097-2765\(00\)80286-5](https://doi.org/10.1016/S1097-2765(00)80286-5)
- Weiss, E. L., 2012 Mitotic exit and separation of mother and daughter cells. *Genetics* 192: 1165–1202. <https://doi.org/10.1534/genetics.112.145516>
- Whinston, E., G. Omerza, A. Singh, C. W. Tio, and E. Winter, 2013 Activation of the Smk1 mitogen-activated protein kinase by developmentally regulated autophosphorylation. *Mol. Cell. Biol.* 33: 688–700. <https://doi.org/10.1128/MCB.00973-12>

Communicating editor: S. Lacefield